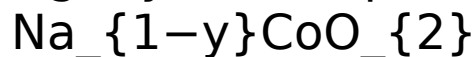




CHORUS

This is the accepted manuscript made available via CHORUS. The article has been published as:

Surface states in lightly hole-doped sodium cobaltate



Meng-Yu Yao, Lin Miao, N. L. Wang, J. H. Dil, M. Z. Hasan, D. D. Guan, C. L. Gao, Canhua Liu, Dong Qian, and Jin-feng Jia

Phys. Rev. B **91**, 161411 — Published 24 April 2015

DOI: [10.1103/PhysRevB.91.161411](https://doi.org/10.1103/PhysRevB.91.161411)

Surface States in Lightly Hole-doped Sodium Cobaltates Na_xCoO_2

Meng-Yu Yao,¹ Lin Miao,¹ N. L. Wang,² J. H. Dil,^{3,4} M. Z. Hasan,⁵ D. D. Guan,^{1,6} C. L. Gao,^{1,6} Canhua Liu,^{1,6} Dong Qian,^{1,6,*} and Jin-feng Jia^{1,6}

¹Key Laboratory of Artificial Structures and Quantum Control (Ministry of Education), Department of Physics and Astronomy, Shanghai Jiao Tong University, Shanghai 200240, China

²International Center for Quantum Materials, School of Physics, Peking University, Beijing 100871, China

³Swiss Light Source, Paul Scherrer Institute, CH-5232 Villigen, Switzerland

⁴Physik-Institut, Universität Zürich, Winterthurerstrasse 190, 8057 Zürich, Switzerland

⁵Department of Physics, Joseph Henry Laboratories, Princeton University, Princeton, New Jersey 08544, USA

⁶Collaborative Innovation Center of Advanced Microstructures, Nanjing 210093, China

(Dated: April 10, 2015)

Using high-resolution angle-resolved photoemission spectroscopy (ARPES), the surface states that were proposed to be useful for constructing the topological superconducting state in sodium cobaltates were experimentally explored. Two energy bands were observed to cross the Fermi level in the large x region. Through *in situ* surface electron doping, temperature dependent ARPES measurements and spin-resolved ARPES measurements, we demonstrated the existence of the surface states due to less Na on the surface than in the bulk as predicted in theory.

Topological superconductors (TSC) can host the exotic quasiparticles named Majorana Fermions (MF)^{1,2}. In recent years many proposals have been raised³⁻¹⁰ including layered Na_xCoO_2 . For example, fractional quantum Hall states³, p-wave superconductors^{4,5}, superconductor-topological insulator(TI) heterostructures^{6,7}, s-wave Rashba superconductors⁸, spin-orbit coupled nodal superconductors⁹, spin-singlet nodal superconductors with magnetic order¹⁰ and so on. Among those proposals, layered cobalt oxide – sodium cobaltate (Na_xCoO_2) is an interesting candidates. For example, in the small x region, superconducting $\text{Na}_{1/3}\text{CoO}_2\cdot\text{H}_2\text{O}$ was proposed to realize nodal d+id TSC¹⁰. In the large x region, Na_1CoO_2 was proposed to form two dimensional (2D) TSC when it is in proximity to a normal s-wave superconductor¹¹.

Without doping ($x=1$), Na_1CoO_2 is a band insulator. Hole-doping was obtained by reducing the Na concentration. Na_xCoO_2 has layered structure and Na atoms locate between the Co-O layers. When cleaving the sample, it breaks at the position where Na^+ ions stay. Na^+ ions on the surface are polar atoms and have large mobility, so some of the ions may leave the surface or move to the sample edges after cleaving. Hence, the hole density on the surface could be different from that in the bulk. Based on this scenario, a recent theory proposed a novel half-metallic SS by reducing the Na concentration on the surface¹¹. In analogy to the s-wave-SC/TI heterostructure, s-wave-SC/ Na_xCoO_2 heterostructure can realize a 2D TSC¹¹. So far, perfect Na_1CoO_2 is not available, however the existence of the surface states in this system should not be limit to the $x=1$ samples. It will be very interesting to know whether there are SS that have the same origin as theory proposed. Experimentally, so far no sign of SS were observed in the small x region ($x < 1/3$)¹⁶⁻²⁰. The measured Fermi surface (FS) area matches the 2D Luttinger count for $x < 1/3$ ^{16,17}, which means the doping level is nearly uniform between the

bulk and the surface. On the other hand, in our previous work¹⁷, we found that the Fermi surface size in the large x ($x \sim 0.7, 0.75, 0.8$) samples did not match the 2D Luttinger count and there were two bands crossing the Fermi level in the very high quality samples. The origin of the double bands was under debate^{21,22}. In this work, we systematically studied the double-band behavior in $x = 0.8 \pm 0.05$ samples by ARPES at varying counter doping of the sample surface with potassium and varying temperature including a spin analysis of the photoelectrons. This revealed that the large Fermi surface originates from the predicted half-metallic surface state exhibiting spin polarization, while the small Fermi surface comes from the spin-degenerate bulk band. Our results move the first step on the way to construct the artificial TSC based on Na_xCoO_2 .

ARPES measurements were carried out using 60-90 eV photons and Scienta analyzers at Advanced Light Source (ALS) beamlines 7.0.1 and 12.0.1 with base pressure better than 2×10^{-11} Torr. The energy resolution is better than 15 meV and angular resolution is better than 1%

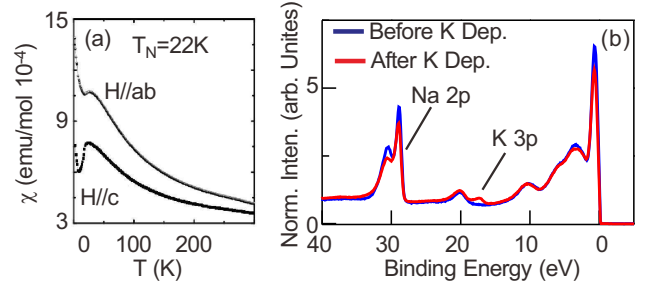


FIG. 1. (a) Magnetic susceptibility $\chi(T)$ of $\text{Na}_{0.8}\text{CoO}_2$. A Néel transition is observed near 22K. (b) The intrinsic Na and extrinsic doped K are carefully checked by the Na-2p and K-3p core level photoemission spectra.

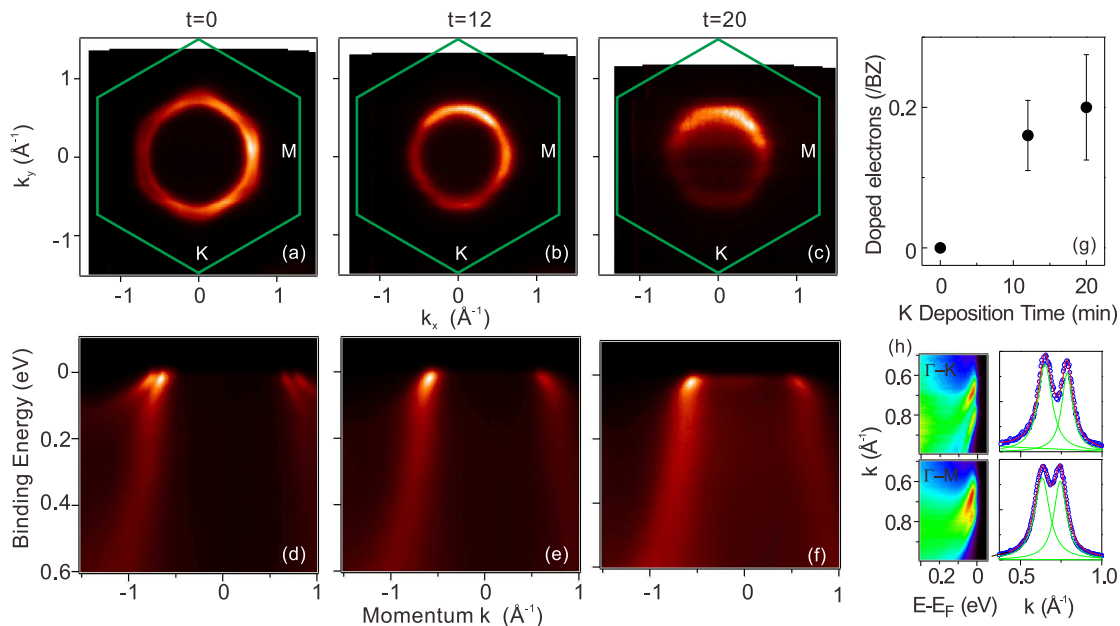


FIG. 2. FS evolution with the electron doping on the surface: (a) Before K deposition, two FS sheets were clearly observed. Green hexagons are the first 2D BZ. FS changed after (b) 12 and (c) 20 minutes K deposition. (d)-(f) is the corresponding momentum cut along $K-\Gamma-K$ direction. (g) Doped electrons in single BZ as a function of K deposition time. (h) High resolution ARPES spectra at $t=0$ along $\Gamma-M$ and $\Gamma-K$ and corresponding MDCs at E_f . MDCs can be fitted by two Lorentzian peaks.

of the Brillouin zone (BZ). Very high quality single crystalline $\text{Na}_{0.8}\text{CoO}_2$ samples were grown by floating zone method. The concentration of Na in the crystals was determined by inductively coupled plasma (ICP) mass spectrometry (iCAP THERMO 6000 Radial). Cleaving the sample *in situ* at $T=15$ K resulted in a shiny surface. Surface electron doping was performed by *in situ* Potassium (K) deposition using Alkali metal dispenser from SAES getters. The nominal K-deposition rate is 0.15 monolayer/min. The sample temperature was kept at 15 K during K-deposition to void any extrinsic thermal effects. Spin-resolved ARPES (SR-ARPES) experiments were carried out at the COPHEE end-station of the SIS beamline, Swiss Light Source (SLS) using 64 eV photons and an Omicron EA 125 hemispherical energy analyzer equipped with two orthogonally mounted classic Mott detectors. The angular and energy resolutions in spin-resolved mode were 1.5° and 60 meV, respectively. Spin-resolved data were taken at 30 K.

Neutron scattering experiments found that long range antiferromagnetic (AFM) order developed below $T_N \sim 20$ K in Na_xCoO_2 with x from 0.25 to 0.1¹². The magnetic moments of Co atoms are ferromagnetic (FM) coupled in the Co-O layer (ab plane) and is AFM coupled between the adjacent Co-O layers. The direction of the magnetic moments is along the c-axis¹³. As shown in Fig. 1 (a), our samples have AFM order below 22 K. Na 2p core-level can be identified at the binding energy of about 30 eV (Fig. 1(b)). Consistent with previous results²⁰, 30.5 eV peak originates from the Na on the surface and 28.5 eV peak comes from the Na in the bulk. Core-level

data imply that there are some Na on the top, but we don't know the exact concentration. K-adsorption was confirmed by K 3p core-level signal (Fig. 1(b)).

The low energy electronic structure near the Fermi energy (E_f) and its evolution as a function of K-coverage are presented in Fig. 2. Fig. 2(a) and (d) show the FS and the quasiparticle spectra along $K-\Gamma-K$ direction before K deposition ($t=0$). Consistent with our previous work¹⁷, the measured FS has two sheets. Both FS sheets are hole pockets known from Fig. 2(d). The inner FS sheet is nearly rounded. The outer FS sheet is hexagonal with corners along $\Gamma-K$ directions. In previous works^{16,17}, FS of $\text{Na}_{1/3}\text{CoO}_2$ is hexagonal with corners along $\Gamma-M$ directions^{16,17,19}. We carefully checked the samples quality with back-scattering Laue diffraction and completely excluded the rotation (30 degree) domains in our samples, so the 30 degree rotation of the outer FS is not due to crystalline quality. Furthermore, according to LDA calculations²⁵, FS of Na_xCoO_2 are always hexagonal with corners along $\Gamma-M$ directions, so the outer FS is not due to the bulk domains with different Na concentration either. Those two bands could be due to bilayer splitting as found in Cuprates²³, or exchange splitting due to in-plane FM order, or surface effect¹¹. Below, using comprehensive experiments, we suggest that the outer FS originates from the surface bands.

With the increase of K coverage, FS changes gradually. Fig. 2 (b) shows the FS after 12 minutes K-deposition. Single FS with weak hexagonal shape was observed. Correspondingly, single band was detected in Fig. 2(e). FS size becomes small with an average $k_f \sim$

0.60\AA^{-1} , which is consistent with the electron doping due to K-deposition. Fig. 2(c) shows the FS after 20 minutes K-deposition. The average k_f becomes $\sim 0.55\text{\AA}^{-1}$. At this stage, FS has well-defined hexagonal shape with corners along $\Gamma - M$ direction, which agrees with the LDA calculations^{24,25}. Based on the size of inner FS, we estimate that roughly 0.2 electrons/BZ were doped into the bulk band after 20 minutes K-deposition(Fig. 2 (g)). The evolution of the FS as a function of surface electron doping can rule out the possibility of bilayer splitting. Bilayer splitting is a bulk property, so surface adsorption can not destroy it.

Momentum distribution curves (MDCs) at E_f along $\Gamma - K - \Gamma$ direction as a function of K-deposition time are shown in Fig. 3 (a). Representative MDCs are shown in Fig. 3 (b). All the spectra are normalized by the photon flux. Due to the matrix element effect, spectra at positive momentum are much clearer, so we focus on positive peaks in MDCs. At $t=0$ minute, there are two peaks (peak position is the Fermi vector k_f) with nearly equal intensity. After exposure to K, before $t=10$ minutes, two peaks both move to the smaller momentum position with different velocity ($v = \Delta k_f / \Delta t$). The outer peak moves faster than the inner peak and two peaks merge eventually. From $t=10$ minutes, only one peak is resolvable but the intensity of this peak becomes higher, which implies the merger of two peaks. After $t=17$ minutes, MDC remains one peak and loses its spectra weight gradually. At the same time, k_f doesn't change, which means no more electrons can be doped into samples. At this stage, some spectra weight around Γ point appears, which should be related to the top of the bulk valence bands shown in LDA calculation^{24,25}. The merger of two bands caused by the surface electron doping provides us three possibilities to understand the two-band behavior. The first possibility is that both bands come from the bulk states. FM order in the Co-O layer can cause the splitting of the low energy bands. Assuming the FM order (within the ARPES detectable depth) can be destroyed by K-deposition, then two bands can merge. The second possibility is that both bands come from ferromagnetic SS. Surface K-deposition may destroy the FM order in SS, which results in the merger of the two bands. The last possibility is the coexistence of the surface and paramagnetic "bulk" states (Paramagnetic "bulk" states are different from the real bulk states. Near surface region, the Co-O layers are possibly paramagnetic.). As discussed below, our temperature dependent ARPES and spin-resolved ARPES experiments support the third possibility.

Figure 4(a)-(f) shows the temperature dependence of the two bands along $\Gamma - K$ direction. The white lines in the figure mark the band dispersion extracted from MDC fitting. With the increase of temperature, both bands become broader and blurred. Though the long range magnetic order forms below 22K, we didn't find any obvious changes below and above 22K in ARPES spectra. At 15 K (Fig. 4(a)) and 50 K (Fig. 4(b)), the

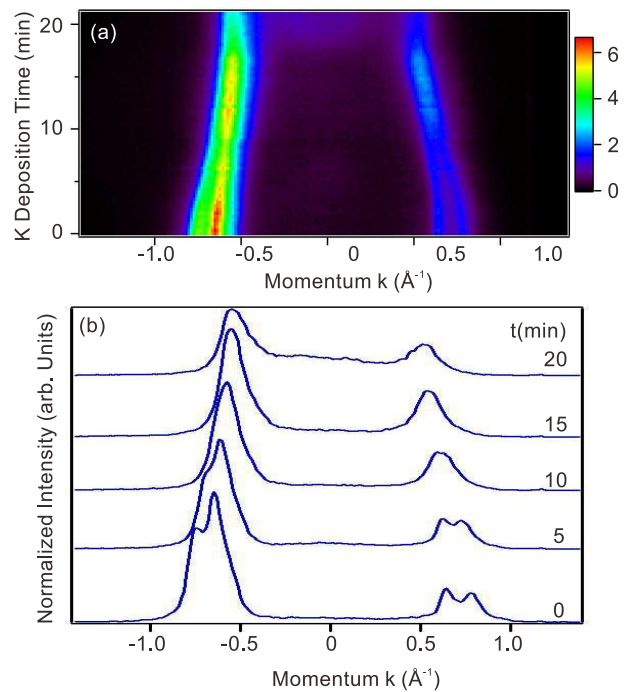


FIG. 3. Time evolution of the quasiparticle bands: (a) Image plot of MDCs at E_f along $K - \Gamma - K$ direction with the increasing of the K-deposition time. (b) Representative MDCs at $t=0,5,15,20$ minutes. Merger of two bands were clearly observed.

band dispersions are the same. According to the neutron scattering, short range FM fluctuations may exist even at 100K^{14,15}. FM fluctuations may cause band splitting, but it should be extremely difficult to detect two nicely dispersive bands because there lacks of long range coherence. In contrast, we detected two well-defined bands even at 200 K. Higher than 200 K, though the features become very broad, two bands are still resolvable. We did MDC fitting at E_f and plotted k_f of the two bands at different temperature in Fig. 4(g). From 15K to 200K, the difference between the k_f of two bands barely changes. Our temperature dependent results strongly suggest that bulk magnetic order plays no role in ARPES spectra. At least, one of the bands should belong to SS. We also did the photon-energy dependence measurements to change the k_z , but it is difficult to distinguish the surface and the bulk bands. Within the experimental uncertainty, both bands are almost k_z independent. Layered structure and bulk AFM states can suppress the bulk k_z dispersion²⁶.

Band dispersions near E_f along two high-symmetry directions ($\Gamma - M$ and $\Gamma - K$) were obtained by MDC fitting(Figure 4(i)). We extracted the energy and k_f differences between the two bands: $\Delta E_{\Gamma-M} \sim 70\text{meV}$, $\Delta k_{f(\Gamma-M)} \sim 0.1\text{\AA}^{-1}$ and $\Delta E_{\Gamma-K} \sim 80\text{meV}$, $\Delta k_{f(\Gamma-K)} \sim 0.15\text{\AA}^{-1}$. ΔE and Δk_f show similar in-plane anisotropy (Fig. 4(j)). Fig. 4(k) and (l) are the LDA calculations (from Ref. [11]) for Na_1CoO_2 including non-magnetic (NM) and FM SS, respectively. One

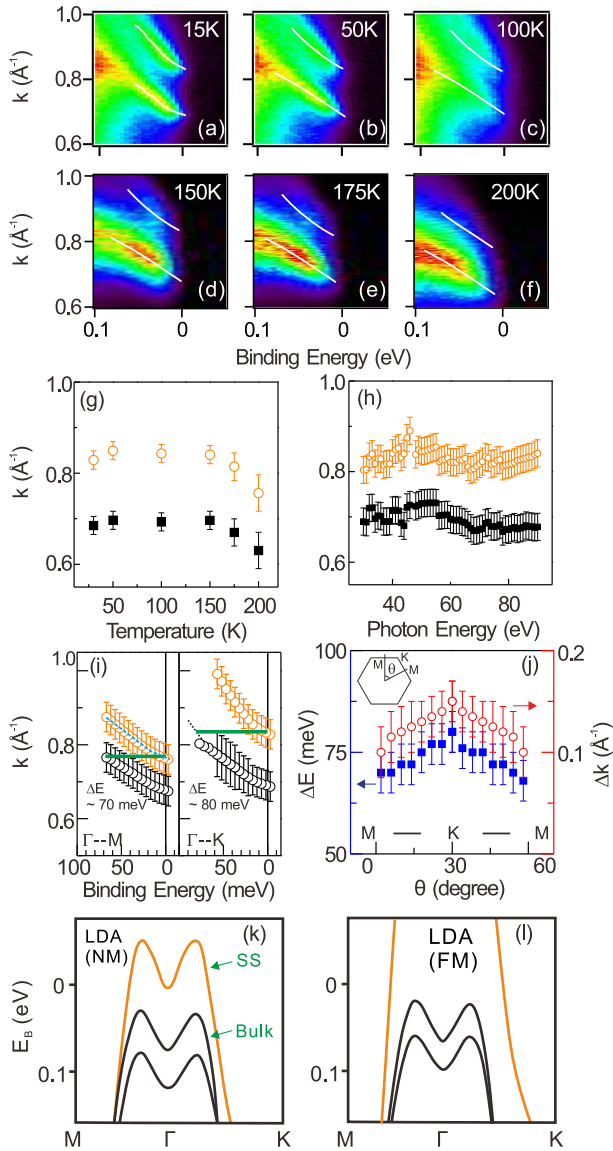


FIG. 4. (a)-(k) Temperature dependence of the quasiparticle bands. Double bands exist at temperature much higher than Néel temperature. (g) Temperature and (h) incident photon-energy dependence of the k_f of the two bands. (i) Dispersion of the low energy bands along the $\Gamma - M$ and $\Gamma - K$ cuts obtained by MDC fittings. Green lines indicate the energy difference between the two bands. Anisotropic (j) Energy and (k) Momentum differences in the BZ. (k) and (l) LDA calculated bands from Ref. [11] under NM and FM states. Black curves are the bulk states. Orange curves are the SS.

notable feature for both NM and FM cases is that the bulk bands and the surface bands are much closer in momentum along $\Gamma - M$ direction than along $\Gamma - K$ direction. In average, for FM case, Δk between the bulk bands and the surface bands is about 0.4 \AA^{-1} and 0.15 \AA^{-1} along $\Gamma - K$ and $\Gamma - M$ direction, respectively. For NM case, it is about 0.1 \AA^{-1} and 0.05 \AA^{-1} . Qualitatively, the experimental anisotropy of the bands (Fig. 4(j)) agrees very

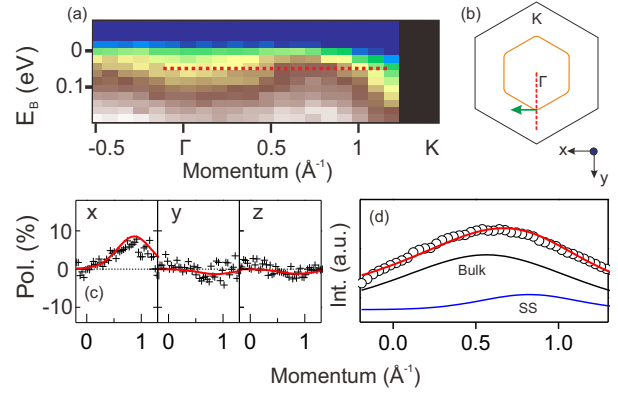


FIG. 5. (a) ARPES spectra in spin-integrated mode. Red dashed line marks the position where spin-resolved MDC was collected. (b) Sketch of the spin direction in the SS. Green arrow presents the spin direction. (c) Measured spin polarization along x, y and z directions. Red line is the fitting curve. (d) MDC and fitting curves.

well with the calculations, which strongly suggest that the outer band is the SS and the inner band is the bulk state. The coexistence of bulk and surface bands can nicely explain the merger of two bands by surface electrons doping in Fig. 3. In calculation¹¹, the hole density is higher on the surface than in the bulk, which causes the SS. By surface electron doping, surface states will get more electron than bulk bands, so the difference of the hole density between surface and bulk becomes weaker and weaker. Eventually surface and bulk becomes the same, so surface and bulk bands completely merge.

Furthermore, we did SR-ARPES measurements. Figure 5(a) shows the spin-integrated ARPES spectra along $\Gamma - K$ direction. Due to the limited energy and momentum resolutions in SR-ARPES beamline comparing to usual ARPES beamline, we can not resolve two bands directly. Instead, two bands are resolved by MDC fitting in spin-resolved mode. We carried out a spin-resolved MDC scan at $E_B = 50 \text{ meV}$. Fig. 5(c) shows the detected spin polarization along x, y and z directions. The detected spin-polarization is small ($\sim 10\%$) and only along +x direction. Experimentally, the spin direction is shown in Fig. 5(b). According to Ref. 11, the in-plane spin component in the NaCoO_2 's SS will rotate in the momentum space anticlockwise when considering the Rashba effect, which means that spin points to Cx direction. Our experimental result is opposite, so we think that the detected spin polarization is not due to Rashba-type spin splitting. The spin direction is also different from the bulk spin states. Under bulk magnetic states, spins are along the c-axis. By a two-step fitting^{27,28}, the MDC and the spin polarization can be fitted as a superposition of a non-spin polarized state and a spin polarized state. We failed to fit the MDC by two states with opposite spins. The fitting results do not support the second possibility that both bands are spin-polarized surface states, though we can not completely rule out this possibility because of

the limited resolution in SR-ARPES. The spin polarized state with larger momentum ($k \sim 0.8\text{\AA}^{-1}$) comes from the outer band and the non-spin polarized state comes from the inner band. Most likely, the inner band is the "bulk" band and the outer band is the SS. SS in our samples is not half-metallic. In the calculation, half-metallic SS is achieved when the flat top of the SS at NM state is located very close to E_f , which depends on the Na concentration on the surface¹¹. In our samples, Fermi level is much lower than Na_1CoO_2 and band top of SS is far away from the Fermi level, so the possible FM coupling and exchange splitting in SS would be much weaker. Ideally, we can hardly detect spin polarization if the exchange splitting is small. The very small spin polarization we detected may be caused by the different ARPES matrix elements of two spin-polarized surface bands. The accurate spin structures of surface bands need to be explored using high-resolution SR-ARPES.

In conclusion, we have reported the existence of SS due to the unequal distribution of hole density near the surface in the lightly hole-doped sodium cobaltates. The

SS is stable and can be slightly tuned by surface electron doping as long as the carrier concentration on the surface is smaller than that in the bulk layers. Though the observed SS is not half-metallic, our findings suggest that the half-metallic SS maybe realized in samples with $x \sim 1$ and it will be very interesting to study the TSC state in superconductor/sodium cobaltates heterostructures in the future.

This work is supported by National Basic Research Program of China (Grants No. 2012CB927401, No. 2011CB921902, No. 2013CB921902, and No. 2011CB922200), NSFC (Grants No. 91021002, No. 10904090, No. 11174199, No. 11227404, and No. 11134008) and the SCST, China (Grants No. 12JC1405300, No. 13QH1401500, No.10JC1407100, No. 10PJ1405700, and No. 11PJ405200). The Advanced Light Source is supported by the Director, Office of Science, Office of Basic Energy Sciences, of the US Department of Energy under Contract No. DE-AC02-05CH11231. D.Q. acknowledges additional supports from the Top-notch Young Talents Program.

* dqian@sjtu.edu.cn

¹ F. Wilczek, Nat. Phys. **5**, 614 (2009).

² J. Alicea, Rep. Prog. Phys. **75**, 076501 (2012).

³ Read and D. Green, Phys. Rev. B **61**, 10267 (2000).

⁴ A. P. Mackenzie and Y. Maeno, Rev. Mod. Phys. **75**, 657 (2003).

⁵ Y. Maeno, S. Kittaka, T. Nomura, S. Yonezawa, and K. Ishida, J. Phys. Soc. Jpn. **81**, 011009 (2012).

⁶ L. Fu, C. L. Kane, Phys. Rev. Lett. **100**, 096407 (2008).

⁷ M.X. Wang, C.H. Liu, J.P. Xu, et. al., Science **336**, 52 (2012).

⁸ J. D. Sau, R. M. Lutchyn, S. Tewari, and S. Das Sarma, Phys. Rev. Lett. **104**, 040502 (2010).

⁹ M. Sato and S. Fujimoto, Phys. Rev. Lett. **105**, 217001 (2010).

¹⁰ Y.M. Lu, Z.Q. Wang, Phys. Rev. Lett. **110**, 096403 (2013).

¹¹ H.M. Weng, G. Xu, H.J. Zhang, S. C. Zhang, X. Dai, Z. Fang, Phys. Rev. B **84**, 060408(R) (2011).

¹² S.P. Bayrakci et al., Phys. Rev. Lett. **94**, 157205 (2005).

¹³ S.P. Bayrakci et al., Phys. Rev. B **69**, 100410(R) (2004).

¹⁴ A.T. Boothroyd et al., Phys. Rev. Lett. **92**, 197201 (2004).

¹⁵ L.M. Helme et al., Phys. Rev. Lett. **94**, 157206 (2005).

¹⁶ H.B. Yang et al., Phys. Rev. Lett. **95**, 146401 (2005)

¹⁷ D. Qian, D. Hsieh, L. Wray, Y.-D. Chuang, et. al., Phys. Rev. Lett. **96**, 216405 (2006).

¹⁸ D. Qian, L. Wray, D. Hsieh, et. al., Phys. Rev. Lett. **97**, 186405 (2006).

¹⁹ T. Shimojima et al., Phys. Rev. Lett. **97**, 267003 (2006).

²⁰ T. Arakane, T. Sato, T. Takahashi, H. Ding, T. Fujii, A. Asamitsu, J. Phy. Soc. Jpn. **76** 054704 (2007).

²¹ D. Qian, D. Hsieh, L. Wray, Y.-D. Chuang, A. Fedorov, L. Viciu, R. J. Cava, and M. Z. Hasan, Phys. Rev. Lett. **101**, 089704 (2008).

²² I. Mazin et al., Phys. Rev. Lett. **101**, 089703 (2008).

²³ D.L. Feng, N.P. Armitage, D.H. Lu, et. al., Phys. Rev. Lett. **86**, 5550 (2001).

²⁴ D.J. Singh, Phys. Rev. B **61**, 13397 (2000).

²⁵ S. Zhou, M. Gao, H. Ding, P. A. Lee, Z. Q. Wang, Phys. Rev. Lett. **94**, 206401 (2005).

²⁶ J. Geck, S.V. Borisenko, H. Berger, et. al., Phys. Rev. Lett. **99**, 046403 (2007).

²⁷ F. Meier, H. Dil, J. Lobo-Checa, L. Patthey, and J. Osterwalder, Phys. Rev. B **79**, 089902 (2009)

²⁸ J. H. Dil, J. Phys.: Condens.Matter **21**, 403001 (2009)